PHYSICAL REVIEW C VOLUME 43, NUMBER 5 MAY 1991

Electroexcitation of negative-parity states in ^{18}O

D. M. Manley
Department of Physics and Center for Nuclear Research, Kent State University, Kent, Ohio 44242

B. L. Berman
Department of Physics, The George Washington University, Washington, D.C. 20052

W. Bertozzi, T. N. Buti,[a] J. M. Finn,[b] F. W. Hersman,[c] C. E. Hyde-Wright,[d] M. V. Hynes,[e] J. J. Kelly,[f] M. A. Kovash,[g] S. Kowalski, R. W. Lourie,[h] B. Murdock,[i] B. E. Norum,[h] B. Pugh,[j] and C. P. Sargent[k]
Department of Physics and Laboratory for Nuclear Science, Massachusetts Institute of Technology, Cambridge, Massachusetts 02139

D. J. Millener
Brookhaven National Laboratory, Upton, New York 11973
(Received 1 November 1990)

Form-factor measurements in the momentum-transfer range $0.6 \leq q \leq 2.7$ fm^{-1} are presented for the 1^- levels in ^{18}O at 4.46, 6.20, 7.62, and 8.04 MeV, the 3^- levels at 5.10, 6.40, and 8.29 MeV, and the 5^- levels at 7.86 and 8.13 MeV. These are the first measurements of the 5^- states by inelastic scattering and the first electron-scattering measurements of the higher 1^- and 3^- states. A Rosenbluth separation of the longitudinal and transverse form factors was performed by fitting the data with a phenomenological polynomial-times-Gaussian parametrization motivated by the form of theoretical form factors when harmonic-oscillator wave functions are used. Comparisons are made with structure models. The Coulomb form factors of several levels indicate the significance of small admixtures of $3\hbar\omega$ components in the negative-parity wave functions.

I. INTRODUCTION

This paper reports an investigation of $T=1$ negative-parity levels in ^{18}O by high-resolution inelastic electron scattering. The work reported here is part of a more comprehensive study of normal-parity excitations in the oxygen isotopes using the (e,e') reaction at the Bates Linear Accelerator Center. High-resolution measurements of inelastic electron scattering to all narrow normal-parity states in ^{16}O up to 12.05 MeV of excitation were reported by Buti *et al.*[1] Measurements of all narrow excited states in ^{17}O up to 15 MeV were reported by Manley *et al.*[2] and high-resolution measurements for the 0^+ levels in ^{18}O at 3.63 and 5.34 MeV, the 2^+ levels at 1.98, 3.92, and 5.26 MeV, and the 4^+ levels at 3.55 and 7.12 MeV were reported previously by Norum *et al.*[3] The first three 4^+ states in ^{18}O and the higher 2^+ levels at 8.21 and 9.36 MeV were discussed recently.[4] We present here form-factor measurements for the 1^- levels at 4.46, 6.20, 7.62, and 8.04 MeV, the 3^- levels at 5.10, 6.40, and 8.29 MeV, and the 5^- levels at 7.86 and 8.13 MeV.

Low-resolution (e,e') measurements ($\sim$250 keV) for the lowest 1^- and 3^- states in ^{18}O were reported previously in a study performed two decades ago at the Saskatchewan electron linear accelerator laboratory.[5] More recently, these states were studied with the (π,π') reaction using (e,e') data from the present work to determine the proton parts of the transition densities.[6] Measurements for the higher 1^- and 3^- states are reported here for the first time. This paper also reports the first study of 5^- states in ^{18}O by inelastic scattering.

The ^{18}O targets and data analysis are described in Secs. II and III. A discussion of individual levels is presented in Sec. IV and a comparison with nuclear-structure calculations is presented in Sec. V. Finally, the results of the present work are summarized in Sec. VI.

II. EXPERIMENTAL PROCEDURE

The $^{18}O(e,e')$ measurements were performed with the Energy-Loss Spectrometer System (ELSSY) at the Bates Linear Accelerator Center. Descriptions of the spectrometer system and focal-plane instrumentation have been presented elsewhere.[7,8] The ^{18}O targets consisted of two isotopically enriched $^9Be^{18}O$ wafers that were manufactured at Lawrence Livermore National Laboratory. The main target had an average thickness of 47.3 mg/cm^2 and abundances of 90.8% ^{18}O, 7.2% ^{16}O, and 2.0% ^{17}O, relative to ^9Be; the other had an average thickness of 21.6 mg/cm^2 and relative isotopic abundances of 46.7% ^{18}O, 52.3% ^{16}O, and 1.0% ^{17}O. Background measurements were acquired by obtaining spectra under identical kinematic conditions with ^9Be, $^9Be^{16}O$, and $^9Be^{17}O$ targets.

Most measurements were performed at a laboratory scattering angle of 90° where Coulomb scattering dominates; however, several additional measurements were performed at 160° to isolate the contributions of the small

transverse form factors. The 90° measurements were performed at incident energies between 119.4 and 268.8 MeV and combined with previous measurements[3] between 90.3 and 369.2 MeV; the 160° measurements were performed at incident energies between 100.5 and 179.5 MeV and combined with previous measurements[3] between 125.4 and 275.2 MeV; one additional 140° measurement was performed at an incident energy of 134.2 MeV. Coulomb form factors were extracted at momentum transfers (q) between 0.6 and 2.7 fm^{-1} for most levels up to about 8.3 MeV of excitation and between 0.9 and 1.9 fm^{-1} for levels between 8.3 and 15 MeV. The energy resolution of the measurements at 90° typically varied from 30 to 40 keV (full width at half maximum) and from 110 to 120 keV at 160°.

Representative spectra that span the excitation region between 4 and 9 MeV (the region of the negative-parity states discussed here) are shown in Fig. 1. The spectrum in the top frame was measured for 194.3-MeV electrons scattered at 90°, corresponding to $q=1.4$ fm^{-1}; the spectrum in the bottom frame was measured at $q=1.8$ fm^{-1}, where high-spin states are evident. The first 5^- state at 7.86 MeV is clearly visible. Coulomb transitions to 5^- states in ^{18}O are interesting because they *must* proceed through (small) $3\hbar\omega$ components in the wave functions of the negative-parity excited states; the main single-particle transitions are $1p\rightarrow 1g$ and $1d\rightarrow 1f$. In the latter case, the transitions proceed through small four-particle, two-hole (4p-2h) components in the ground-state wave function.

III. DATA ANALYSIS

Absolute differential cross sections were obtained from the measured spectra by using a line-shape fitting procedure that has been described previously.[1] The extracted form factors were renormalized (by 10% or less) relative to known elastic cross sections for ^{18}O to compensate for uncertainties due to fluctuations in target thickness, beam monitoring, etc.

The differential cross section for inelastic electron scattering in the plane-wave Born approximation (PWBA) is given by[9]

$$\frac{d\sigma}{d\Omega}=Z^2\sigma_{\text{Mott}}\eta\left\{\frac{Q^4}{q^4}|F_L(q)|^2+\left[\frac{Q^2}{2q^2}+\tan^2\left[\frac{\theta}{2}\right]\right]|F_T(q)|^2\right\}, \quad (1)$$

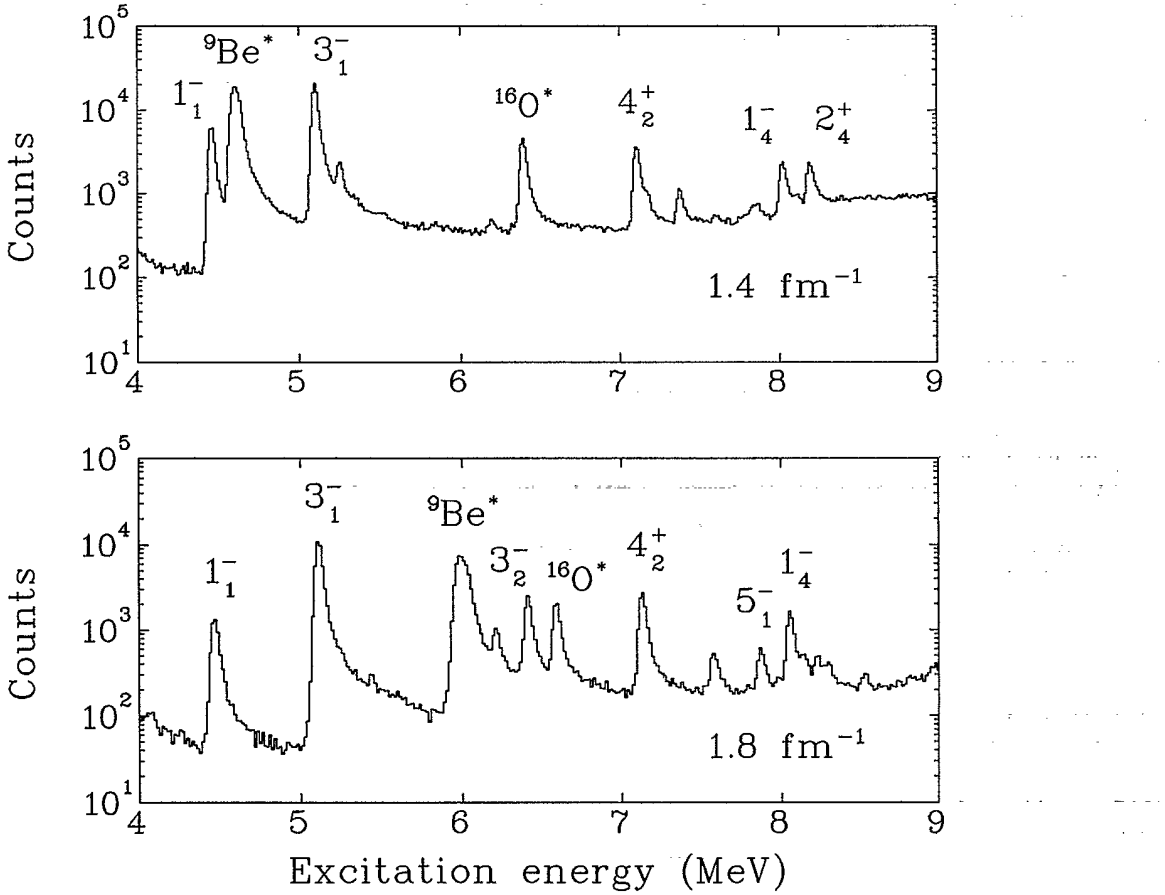

FIG. 1. Top frame: a spectrum for electrons scattered from ^{9}Be^{18}O at $E_0=194.3$ MeV and $\theta=90°$, corresponding to $q=1.4$ fm^{-1}. The 3^-_2 state at 6.40 MeV is obscured by the 3^-_1 state in ^{16}O at 6.13 MeV (labeled ^{16}O*). Bottom frame: a spectrum for electrons scattered from ^{9}Be^{18}O at $E_0=248.4$ MeV and $\theta=90°$, corresponding to $q=1.8$ fm^{-1}. (The label ^{9}Be* indicates the $\frac{5}{2}^-$ state in ^{9}Be at 2.43 MeV.) Note the relative enhancement of the 5^-_1 state at 7.86 MeV as q increases.

where Z is the nuclear charge,

$$\sigma_{\text{Mott}}=\left[\frac{\alpha}{2E_0}\right]^2\frac{\cos^2(\theta/2)}{\sin^4(\theta/2)} \tag{2}$$

is the Mott cross section, α is the fine-structure constant, E_0 is the incident electron energy, θ is the laboratory scattering angle, q is the three-momentum transfer, $Q^2=q^2-\omega^2$ is the square of the four-momentum transfer, $\omega=[(M+E_x)^2+q^2]^{1/2}-M$ is the electron energy loss, M is the mass of the target nucleus, E_x is the excitation energy of the recoil nucleus, and

$$\eta=\left[1+\frac{2E_0}{M}\sin^2\left[\frac{\theta}{2}\right]\right]^{-1} \tag{3}$$

is the target recoil factor. For the kinematics of the present measurements, $\eta\approx 1$ and $Q^2/q^2\approx 1$. If the target nucleus is spinless, then for the excitation of normal-parity states with spin J we can write $F_L(q)=E_{CJ}(q)$ and $F_T(q)=F_{EJ}(q)$, where $F_{CJ}(q)$ is the longitudinal electric or Coulomb form factor and $F_{EJ}(q)$ is the transverse electric form factor. A first-order correction for distortion of the scattered electron waves by the nuclear Coulomb field was made by replacing q with the effective momentum transfer q_{eff} defined by

$$q_{\text{eff}}=q\left[1-\frac{V_C(r)}{E_0}\right]. \tag{4}$$

Here $V_C(r)$ is the nuclear Coulomb field at $r=(J+1)/q$, a distance that approximates the innermost peak of the overlap between incident and outgoing partial waves.[10] For simplicity, the nuclear Coulomb field was approximated by that of a uniformly charged sphere of radius $\sqrt{(5/3)}1.2A^{1/3}$ fm.

Measurements of total form factors,

$$|F|^2=(Z^2\sigma_{\text{Mott}}\eta)^{-1}\frac{d\sigma}{d\Omega}, \tag{5}$$

are available from the Physics Auxiliary Publication Service (PAPS).[11] Data are tabulated for all of the normal-parity excited states in ^{18}O below 9 MeV, including previously unpublished form-factor data extracted from the (e,e') measurements discussed in Ref. 3. Also tabulated are (sparse) data for normal-parity states at 9.36, 9.71, 10.29, 11.65, and 12.04 MeV.

The form-factor measurements for exciting normal-parity states with spin J were parametrized by a polynomial-times-Gaussian (PG) form:

$$F_{CJ}(q)=\frac{\sqrt{4\pi}}{Z}\frac{q^J}{(2J+1)!!}f_{\text{c.m.}}(q)f_N(q)\times e^{-y}\sum_{n=0}^{N}A_n y^n, \tag{6}$$

$$F_{EJ}(q)=\frac{\sqrt{4\pi}}{Z}\frac{q^J}{(2J+1)!!}\left[\frac{J+1}{J}\right]^{1/2}\times\frac{\omega}{q}f_{\text{c.m.}}(q)f_N(q)e^{-y}\sum_{n=0}^{N+1}B_n y^n, \tag{7}$$

where A_n and B_n were treated as variable coefficients. Note that for normal-parity excitations, consistency with the continuity equation requires $A_0=B_0\approx\sqrt{B(CJ)\uparrow}$. The PG parametrization was chosen to facilitate comparisons with shell-model calculations that use harmonic-oscillator wave functions.[12] The number of coefficients is a reflection of the model space; for a single-particle transition between major shells with N_i and N_f oscillator quanta, respectively, the summation in Eq. (6) extends up to $N=0.5\ [(N_i+N_f)_{\max}-J]$. The factor $f_{\text{c.m.}}=\exp(y/A)$ is the harmonic-oscillator "center-of-mass" correction for the lack of translational invariance in shell-model wave functions, A is the atomic weight of the target, the dimensionless parameter y is defined as $y=(qb/2)^2$, and b is the harmonic-oscillator length parameter. Also, $f_N(q)=(1+q^2/\Lambda^2)^{-2}$ is the dipole form factor that corrects for finite nucleon size with $\Lambda=4.33$ fm^{-1}, which corresponds to a proton charge radius of 0.80 fm.

A Rosenbluth separation of the longitudinal and transverse form factors was achieved by fitting form-factor measurements according to the prescription above. "Experimental" data points for the separated longitudinal (transverse) form factor were obtained from individual measurements of the total form factor by subtracting the fitted transverse (longitudinal) contribution. In this manner, Coulomb form factors were extracted from measurements taken at $\theta=90°$ and transverse form factors were extracted from measurements taken at $\theta>90°$.

Form-factor measurements for 15 normal-parity states of established spin and parity ($J^\pi=1^-$, 2^+, 3^-, 4^+, and 5^-) were fitted simultaneously subject to the constraint that the oscillator parameter b have the same value for all states. The fitted value $b=1.879\pm0.023$ fm is about 3% larger than the value 1.821 fm extracted[13] from the experimental rms charge radius 2.794 ± 0.005 fm.[14] (The quoted uncertainty in the oscillator constant is three times the statistical uncertainty; see Sec. V.) Table I lists the fitted values of the expansion coefficients A_n and B_n [defined in Eqs. (6) and (7)] for all of the states except the 3_3^- state at 8.29 MeV, for which the cross section was too small to determine meaningful coefficients.

The PWBA Coulomb form factor $F_{CJ}(q)$ is related to the transition charge density $\rho_J(r)$ by[9]

$$F_{CJ}(q)=\frac{\sqrt{4\pi}}{Z}\frac{\hat{J}_f}{\hat{J}_i}\int_0^\infty j_J(qr)\rho_J(r)r^2dr, \tag{8}$$

where $\hat{J}=\sqrt{2J+1}$ and $j_J(qr)$ is a spherical Bessel function. [For ^{18}O, $J_i=0$ and $J_f=J$. It should be noted that some authors normalize transition densities differently than given by Eq. (8)]. If harmonic-oscillator wave functions are used, the transition densities will have a PG form given by

$$\rho_J(r)=b^{-3}x^J e^{-x^2}\sum_{n=0}^{N}C_n x^{2n}, \tag{9}$$

where $x=r/b$. The form factors derived from this parametrization have the form given by Eq. (6), but with the factor $f_{\text{c.m.}}f_N$ replaced by unity. Transition charge

TABLE I. Expansion coefficients (in e fm^J) for the longitudinal and transverse electric form factors of selected normal-parity states in ^{18}O. (Only the uncertainties due to fitting are represented.) The value of the oscillator parameter b is 1.879(23) fm. (Uncertainties in the last significant figure are given in parentheses and values in square brackets were not varied.)

J_n^π	E_x (MeV)	A_0	A_1	A_2	B_1	B_2
1_1^-	4.46	0.044(21)	−1.044(26)	0.245(5)	1.40(46)	−2.48(17)
1_2^-	6.20	[0.0468]	−0.135(13)	0.117(5)	0.08(24)	0.65(15)
1_3^-	7.62	[0.025]	−0.070(37)	0.037(12)	−0.53(28)	−0.19(17)
1_4^-	8.04	[0.031]	−0.407(11)	0.015(6)	0.5(18)	−0.2(17)
2_1^+	1.98	6.392(51)	−1.062(85)	−0.256(18)	−10.4(94)	4.7(29)
2_2^+	3.92	4.591(39)	−1.940(49)	0.009(12)	0.6(28)	−1.6(11)
2_3^+	5.26	5.348(52)	−2.254(59)	0.099(13)	−0.8(15)	0.7(7)
2_4^+	8.21	2.71(26)	−0.33(30)	−0.080(79)	−8.6(43)	3.9(17)
3_1^-	5.10	36.10(18)	−1.31(28)		−39.8(94)	
3_2^-	6.40	6.31(23)	2.63(20)		28.1(34)	
4_1^+	3.56	31.12(56)	−1.38(24)		94(15)	
4_2^+	7.12	113.8(15)	−13.14(59)		−55(81)	
5_1^-	7.86	188.4(57)			−390(160)	
5_2^-	8.13	137.4(42)			−290(180)	

densities were extracted by refitting the data, as discussed already, but with this modification to the fitting function. The fitted form factors obtained by this procedure did not differ significantly from those obtained using the form given by Eq. (6). It is sometimes useful to extract *point-proton* transition densities by fitting the data with the form given by Eq. (6), but with only the factor $f_{\text{c.m.}}$ replaced by unity. Table II lists the expansion coefficients C_n for the point-proton densities of the negative-parity states.

IV. RESULTS AND DISCUSSION

In the discussion that follows, the extracted Coulomb form factors for the low-lying 1^-, 3^-, and 5^- states in ^{18}O are described and arguments are presented for the evidence of $3\hbar\omega$ admixtures in their wave functions. To help understand these arguments, we briefly describe here the various components that may arise in the negative-parity wave functions if the model space for the positive-parity states is allowed to contain $2\hbar\omega$ components.

The wave functions of the positive-parity states will be of the form

$$|\pi=+\rangle=\alpha_0|(sd)^2\rangle+\beta_2|p^{-2}(sd)^4\rangle+\gamma_2|p^{-1}(sd)^2(pf)\rangle+\delta_2|s^{-1}(sd)^3\rangle+\varepsilon_2|(sd)(sdg)\rangle+\zeta_2|(pf)^2\rangle\ , \tag{10}$$

if one includes $2\hbar\omega$ components. Small amplitudes $(\gamma_2,\delta_2,\varepsilon_2)$ of 1p-1h $2\hbar\omega$ configurations, corresponding to the giant quadrupole resonances, are well known to provide the major source of enhancement to $C2$ matrix elements. From Eq. (10) it follows that the wave functions of the negative-parity states will be of the form

TABLE II. Expansion coefficients for the point-proton transition densities of selected negative-parity states in ^{18}O. (Only the uncertainties due to fitting are represented.) The value of the oscillator parameter b is 1.824(23) fm. (Uncertainties in the last significant figure are given in parentheses.)

J_n^π	E_x (MeV)	C_0	C_1	C_2
1_1^-	4.46	−0.147(46)	−0.391(24)	0.1309(28)
1_2^-	6.20	0.399(28)	−0.367(19)	0.0620(26)
1_3^-	7.62	0.097(78)	−0.104(52)	0.0199(66)
1_4^-	8.04	−0.423(35)	0.145(24)	0.0087(31)
3_1^-	5.10	0.316(15)	0.0155(32)	
3_2^-	6.40	0.200(10)	−0.0295(22)	
5_1^-	7.86	0.019 43(54)		
5_2^-	8.13	0.014 17(57)		

$$|\pi=-\rangle=\alpha_1|p^{-1}(sd)^3\rangle+\beta_1|(sd)(pf)\rangle+\gamma_3|p^{-3}(sd)^5\rangle+\delta_3|p^{-2}(sd)^3(pf)\rangle+\varepsilon_3|p^{-1}(sd)(pf)^2\rangle+\zeta_3|s^{-1}p^{-1}(sd)^4\rangle$$
$$+\eta_3|s^{-1}(sd)^2(pf)\rangle+\kappa_3|p^{-1}(sd)^2(sdg)\rangle+\nu_3|(pf)(sdg)\rangle+\xi_3|(sd)(pfh)\rangle\ . \qquad (11)$$

We note that the prohibitive number of equivalent (in unperturbed excitation energy) components in the negative-parity wave functions presents a challenge to any structure-model calculation and indicates the necessity of a reasonable truncation scheme. Now consider matrix elements in which the positive-parity ground state is connected to a negative-parity excited state through a one-body operator. Clearly, the most important matrix elements are those that involve α_0 or β_2 in Eq. (10). The simplest excitations to consider are the 5^- states. Unlike the 1^- and 3^- states that are excited primarily by $1\hbar\omega$ $p\rightarrow sd$ transitions, 5^- Coulomb (i.e., proton) excitations are excited primarily by $1\hbar\omega$ $1d\rightarrow 1f$ transitions (via the $\beta_2\delta_3$ term) and $3\hbar\omega$ $1p\rightarrow 1g$ transitions (via the $\alpha_0\kappa_3$ term). If one assumes that $|\delta_3|\approx|\kappa_3|$, then the $1p\rightarrow 1g$ transitions are expected to be the dominant mechanism for the 5^- Coulomb excitations ($\alpha_0\sim 2\beta_2$ also helps), basically because the full p shell is available to make transitions as opposed to a small fraction of the full d shell.

For the 1^- and 3^- excitations, we observe deviations in the shapes of their Coulomb form factors, which are discussed below and cannot be explained by the dominant $p\rightarrow sd$ transitions for these states; these shape deviations most likely result from $p\rightarrow sdg$ transitions, which we argue are mainly responsible for the 5^- Coulomb excitations. We note, however, that small $sd\rightarrow pf$ proton amplitudes also may contribute from core polarization of the ground state.

Figure 2 shows transition charge densities derived from fitting form-factor measurements for the negative-parity states as discussed in Sec. III; hatched areas represent error bands. (For plotting purposes the densities have been scaled such that they are all positive as r approaches zero.) The densities are well determined for the 1^- levels at 4.46, 6.20, and 8.04 MeV and for the 3^- states at 5.10 and 6.40 MeV; the very small cross section for the 3_3^- state at 8.29 MeV precluded the extraction of a meaningful transition density. The 1^- densities are qualitatively similar although the densities of the 1_2^- and 1_4^- states peak at a smaller radius than that of the 1_1^- state. The 3^- densities have similar shapes but different strengths. The densities for the 1_4^- and 3_1^- levels are characteristic of fairly pure $p\rightarrow sd$ excitations. The relatively large error envelopes for the 5^- states reflect the lack of accurate low-q data for these states and the strong correlation between their expansion coefficients and the oscillator parameter.

A. 1^- levels

Figure 3 shows the extracted Coulomb form factors for the first four 1^- states. The curves were generated by fitting the measurements as described in the preceding section but with A_0 and B_0 constrained to agree with the $B(C1)\uparrow$ values deduced from independent information on their electromagnetic decays. For the 4.46-MeV level, we find $B(E1)\downarrow<3.0\times10^{-6}$ W.u. (where W.u. represents Weisskopf unit), based on a mean lifetime of 65±15 fs (Ref. 15) and a ground-state branching ratio of $<1\%$.[16] The mean lifetime of the 6.20-MeV level is 3.22±0.54 fs, based on a ground-state transition width of 180±30 meV and a ground-state branching ratio of 88±3%.[17] From these values we find $B(E1)\downarrow=(1.65\pm0.27)\times10^{-3}$ W.u.; this value is not significantly affected by a more recent determination of the ground-state branching ratio to be 88.7±0.9%.[15] Gai *et al.* have measured $B(E1)\downarrow=(4.6\pm1.0)\times10^{-4}$ W.u. for the 7.62-MeV level and $B(E1)\downarrow=(7.2\pm1.5)\times10^{-4}$ W.u. for the 8.04-MeV level.[18] For $E1$ transitions in ^{18}O, 1 W.u.$=0.443\ e^2\,\mathrm{fm}^2$. Table III summarizes the corresponding $B(E1)\uparrow$ values and the inferred values of the expansion coefficients A_0 and B_0 for the 1^- states.

Shell-model calculations that use the complete $1\hbar\omega$ space of $p^{-1}(sd)^3$ plus $(sd)(pf)$ configurations predict low-lying 1^- states in ^{18}O at 4.46, 6.83, 7.63, and 8.21 MeV, where the energy of the lowest state has been shifted to agree with the experimental value. These calculations, discussed in Sec. V, show that the $(sd)(pf)$ components are small for most states. The $B(E1)\downarrow$ values predicted for the four 1^- states are 2.9×10^{-5}, 2.0×10^{-3}, 4.5×10^{-3}, and 7.9×10^{-2} W.u., respectively. The strong hindrance of the transition from the first 1^- state is well reproduced, as is the transition strength for the second state, but the transition strengths for the remaining states, particularly the fourth state, are much too large.

The $C1$ form factor of the 1_1^- state at 4.46 MeV is well sampled over the effective momentum-transfer range 0.7–2.6 fm^{-1}. The locations of the first two maxima at 1.1 and 2.5 fm^{-1} and the diffraction minimum at 2.2 fm^{-1} are well determined. In the measured momentum-transfer range, the transverse form factor has a single maximum at 1.5 fm^{-1}. The experimental $\sigma(\pi^+)/\sigma(\pi^-)$ ratio is 1.3±0.2 for the 4.46-MeV state,[6] which indicates

TABLE III. Reduced transition probabilities for the low-lying 1^- levels in ^{18}O. The values were determined from electromagnetic lifetimes and branching fractions as described in the text. Also listed are the inferred values of the expansion coefficients (given by the square roots of values in column 4) that were used to constrain fits of the (e,e') data.

J_n^π	E_x (MeV)	$B(E1)\downarrow$ (W.u.)	$B(E1)\uparrow$ ($e^2\,\mathrm{fm}^2$)	A_0 or B_0 (e fm)
1_1^-	4.46	$<3\times10^{-6}$	$<4\times10^{-6}$	<0.002
1_2^-	6.20	$1.65(27)\times10^{-3}$	$2.19(36)\times10^{-3}$	0.0468(38)
1_3^-	7.62	$4.6(10)\times10^{-4}$	$6.1(13)\times10^{-4}$	0.025(3)
1_4^-	8.04	$7.2(15)\times10^{-4}$	$9.6(20)\times10^{-4}$	0.031(3)

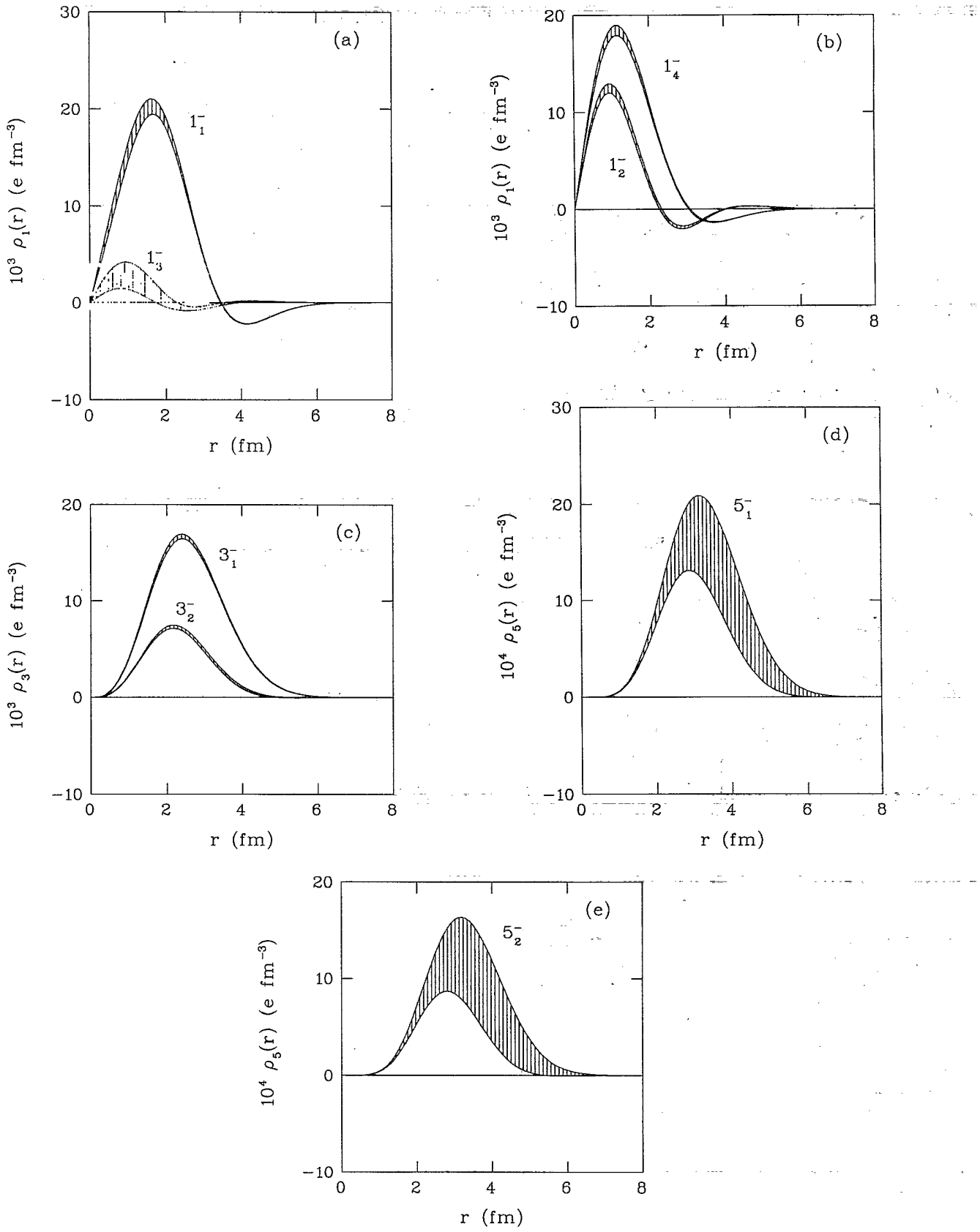

FIG. 2. Transition charge densities extracted for (a) the 1_1^- state at 4.46 MeV and the 1_3^- state at 7.62 MeV, (b) the 1_2^- state at 6.20 MeV and the 1_4^- state at 8.04 MeV, (c) the 3_1^- state at 5.10 MeV and the 3_2^- state at 6.40 MeV, (d) the 5_1^- state at 7.86 MeV, and (e) the 5_2^- state at 8.13 MeV. The hatched areas represent error bands.

that the transition to this state is strongly isoscalar; thus, as might be expected, the strengths and shapes of the longitudinal and transverse form factors for this state are similar to those of the 1_1^- state at 7.12 MeV in ^{16}O.[1] The main difference is that a second maximum is not observed below 3 fm^{-1} in the $C1$ form factor of the 7.12-MeV state.

The $C1$ form factor of the 1_2^- state at 6.20 MeV is measured over the momentum-transfer range 1.3–2.6 fm^{-1}. Reliable measurements could not be extracted at lower q because the relevant (e,e') spectra in the vicinity of the 6.20-MeV level are dominated by a strong contaminant peak from the 3_1^- state in ^{16}O. The momentum-transfer region of our measurements is dominated by what probably is the second maximum. (Our fit suggests that the first maximum occurs at about 0.4 fm^{-1}.) This state has a small but measurable transverse form factor. Interestingly, the shell-model calculations show that the predicted level at 6.83 MeV (identified with the experimental level at 6.20 MeV) has a fairly large $(sd)(pf)$ component

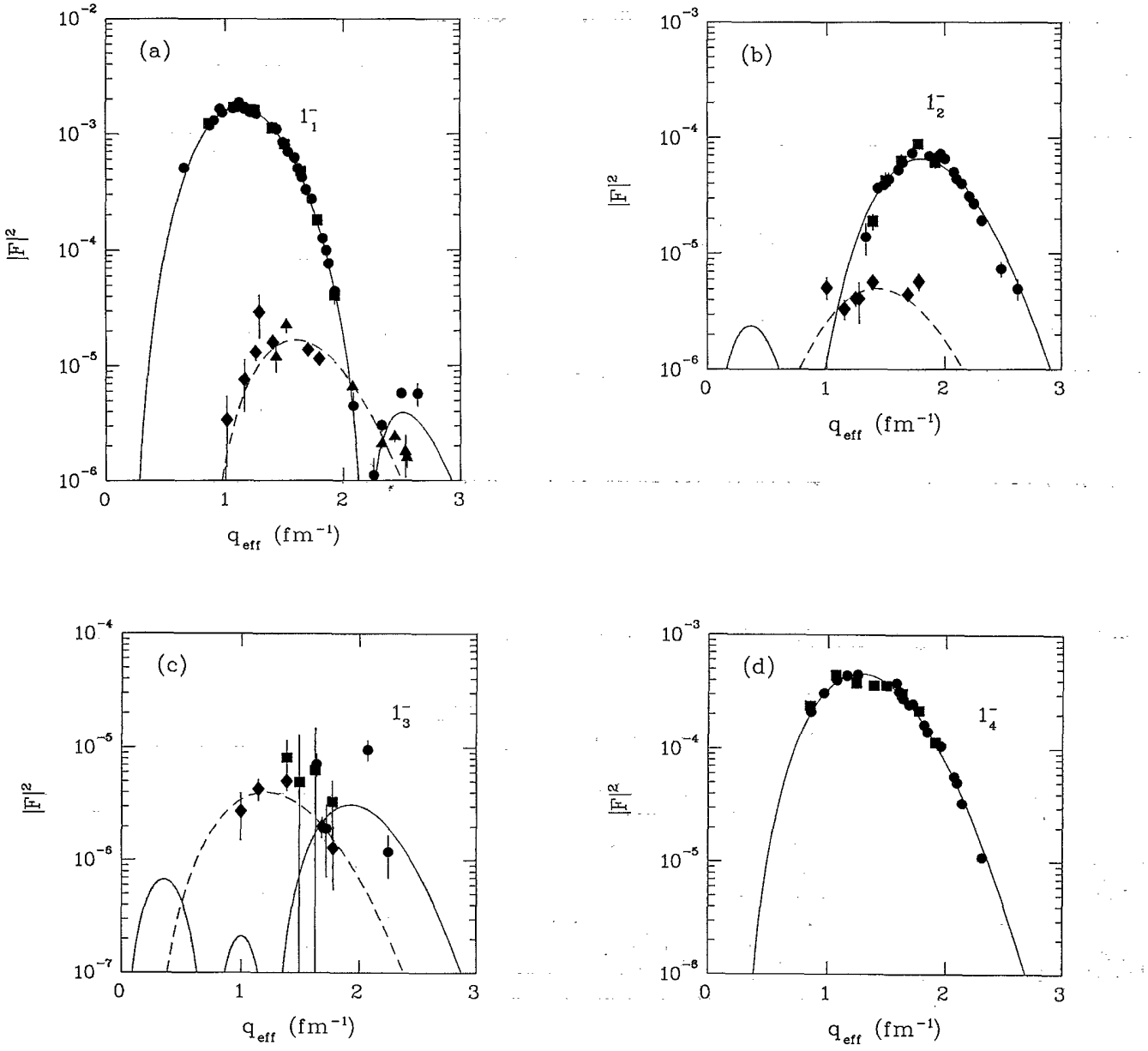

FIG. 3. Extracted Coulomb (solid lines) and transverse electric (dashed lines) form factors for 1^- states in ^{18}O at excitation energies of (a) 4.46 MeV (1_1^-), (b) 6.20 MeV (1_2^-), (c) 7.62 MeV (1_3^-), and (d) 8.04 MeV (1_4^-). Solid squares (diamonds) indicate measurements of longitudinal (transverse) form factors from the present analysis, and solid circles (triangles) indicate measurements from an earlier analysis (see text).

(17.9%) in its wave function.

The $C1$ form factor of the 1_3^- state at 7.62 MeV is small ($<10^{-5}$) and very poorly determined by our measurements; however, our measurements suggest that this state has a significant transverse form factor.

Our form-factor measurements for the 1_4^- state at 8.04 MeV determine its $C1$ form factor between 0.9 and 2.3 fm^{-1}; the shape of its Coulomb form factor is very similar to that of the 3_1^- state in ^{18}O, which indicates that the transition is strongly dominated by a $p \rightarrow sd$ proton amplitude (see below). Unlike the lower 1^- states at 4.46, 6.20, and 7.62 MeV, the 8.04-MeV level has (within experimental uncertainties) a negligible transverse form factor.

Interestingly, the $C1$ form factors for the 1_1^- states in both ^{16}O and ^{18}O cannot be fitted adequately (with the PG parametrization) if only expansion coefficients associated with $p \rightarrow sd$ transitions are allowed to vary.[6] The $C1$ form factor for a 1^- level with negligible $B(C1)\uparrow$ is expected to vary like $F_{C1} \propto y^{3/2}e^{-y}$, if the state arises strictly from $1p \rightarrow 1d$ and $1p \rightarrow 2s$ transitions [which then occur in the combination corresponding to the SU_3 amplitude for $(\lambda\mu)=(21)$ with $\Delta L=1$ and $\Delta S=0$]. Although this shape describes the 1^- level at 8.04 MeV well, the form factors for the levels at 4.46 and 6.20 MeV are given approximately by $F_{C1} \propto y^{3/2}(1-cy)e^{-y}$, where $c=0.23$ and 0.87, respectively (see Table I). The additional $y^{5/2}$ terms probably arise from $3\hbar\omega$ $1p \rightarrow 2d$ and $1p \rightarrow 3s$ proton transitions that proceed through small components in the wave functions of the low-lying 1^- levels (see Sec. V B).

B. 3^- levels

Figure 4 shows the extracted Coulomb form factors for the three 3^- states that lie lowest in energy. Transverse form factors of these states are negligible, within experimental uncertainties. The experimental $\sigma(\pi^+)/\sigma(\pi^-)$ ratio of nearly 1.0 for the 3_1^- state at 5.10 MeV (Ref. 6) indicates that the transition to this state is mainly isoscalar. The $C3$ form factor of the 5.10-MeV state is strikingly similar to that of the 3_1^- state at 6.13 MeV in ^{16}O.[1] This result is not surprising since harmonic-oscillator shell-model calculations that describe the excitation of 3^- states as arising from $1p \rightarrow 1d$ transition predict all $C3$ form factors to have a shape given by $F_{C3} \propto y^{3/2}e^{-y}$. In general, for transitions with $J=(N_i+N_f)_{\max}$, the Coulomb form factor behaves as $F_{CJ} \propto y^{J/2}e^{-y}$ (see Sec. III).

It is clear from Fig. 4 that the $C3$ form factor of the 3_2^- state at 6.40 MeV differs from that of the 3_1^- state; maxima in the $C3$ form factors of the 3_1^- and 3_2^- states occur at 1.3 and 1.5 fm^{-1}, respectively. Shape differences among the $C3$ form factors for these 3^- states indicate the active participation of orbitals beyond the *sd* shell; the most important shape changes probably come from $1p \rightarrow 1g$ and $1p \rightarrow 2d$ proton transitions (see Sec. V B).

The shape of the $C3$ form factor for the weakly excited 3_3^- state at 8.29 MeV is not well determined by the present measurements except perhaps at high momentum transfer. The shell-model calculations already mentioned show that the third predicted 3^- state (identified with the experimental level at 8.29 MeV) has a fairly large $(sd)(pf)$ component (16.4%) in its wave function.

C. 5^- levels

The extracted Coulomb form factors of the first two 5^- states at 7.86 and 8.13 MeV are shown in Fig. 5. The extracted transverse form factors are negligible for both states, within experimental uncertainties. These measurements are of interest because they provide direct evidence for high-spin negative-parity excitations that cannot arise from simple $p \rightarrow sd$ transitions. Coulomb excitations of low-lying 2^+ and 4^+ states in ^{18}O are well known to proceed mainly through $2\hbar\omega$ components in the wave functions of the ground state and positive-parity excited states; by analogy, the Coulomb excitation of 5^- states proceeds through $3\hbar\omega$ components in the wave functions of the negative-parity excited states. If we assume that the 5^- states arise strictly from isoscalar $1p \rightarrow 1g$ transitions, then a simple calculation (see Sec. V B) shows that the two states together exhaust about 7% of the sum-rule strength.

In Ref. 3 it was stated that the level at 7.86 MeV might be a 4^+ state. Since 4^+ states in ^{18}O are excited by $1d \rightarrow 1d$ and $1p \rightarrow 1f$ transitions, the shape of their Coulomb form factors should be given by $F_{C4} \propto y^2e^{-y}$; similarly, Coulomb form factors for 5^- states in ^{18}O should be given by $F_{C5} \propto y^{5/2}e^{-y}$ because such states are excited primarily by $1p \rightarrow 1g$ and $1d \rightarrow 1f$ transitions. Figure 5 shows that the level at 7.86 MeV has a maximum at about 1.6 fm^{-1}, as does the established 5^- state at 8.13 MeV. For comparison, Fig. 6 shows that the maxima for the first two 4^+ states at 3.56 and 7.12 MeV occur at about 1.4 fm^{-1}; hence, the electron-scattering data presented here support the conclusion of Gai *et al.*[18] that the level at 7.86 MeV is indeed a 5^- state.

D. Reduced transition probabilities

By making extrapolations to the photon point, it is often possible to deduce reduced Coulomb transition probabilities, which are moments of the transition charge density. In Table IV we present values for reduced transition probabilities that were obtained by fitting form-factor measurements with the parametrizations discussed in Sec. III. The uncertainties given in Table IV are three times larger than those implied by the statistical uncertainties in Table I. The larger values attempt to take into account not only the statistical uncertainties but also the model dependency of our parametrization and the fact that there are no data points for $q_{\text{eff}}<0.64$ fm^{-1}; based on several fits performed with different numbers of expansion coefficients and different values of the oscillator parameter, we believe that the uncertainties given in Table IV are reasonable. Some confidence in our values may be obtained by noting that the $B(C2)\uparrow$ and $B(C4)\uparrow$ values given here (which are not intended to supersede

those of Ref. 3) agree, on the average, with those in Ref. 3 to within about 5%. The $B(C3)\uparrow$ value for the 3_1^- state obtained in the present work is about 15% larger than that obtained from low-q measurements performed at the Saskatchewan electron linear accelerator.[5] It may also be noted that our $B(C3)\uparrow$ value for the 3_1^- state in ^{18}O is only about 10% smaller than the value $1411\pm28\ e^2\,\mathrm{fm}^6$ determined for the 3_1^- state in ^{16}O.[1]

The theoretical $B(C2)\uparrow$ and $B(C4)\uparrow$ values listed in Table IV are based on models[4,19] that empirically mix $(sd)^2$ and $p^{-2}(sd)^4$ shell-model eigenstates in the spirit of the model of Lawson, Serduke, and Fortune.[21] In this case there are delicate interferences between the matrix elements connecting 2p-0h states and those connecting 4p-2h states (which can be related to matrix elements within the ^{20}Ne ground-state band) but the matrix elements connecting $0\hbar\omega$ and $2\hbar\omega$ configurations are negligible, such effects having been subsumed into the effective charges. For $C1$ and $C3$ transitions, the situation is different when the ground state contains 4p-2h components in that the $0\hbar\omega\rightarrow 1\hbar\omega$ and $2\hbar\omega\rightarrow 1\hbar\omega$ contributions can interfere directly. However, the $2\hbar\omega$ admixtures included in the ground-state wave function in the models above include only a small fraction of octupole-octupole configurations, for example, built on the $0\hbar\omega$ part of the ground-state wave function.

V. COMPARISONS WITH NUCLEAR-STRUCTURE CALCULATIONS

The shell-model calculation that we use as a basis for discussion of the negative-parity states of ^{18}O employs the full, nonspurious $1\hbar\omega$ basis of $p^{-1}(sd)^3$ and $(sd)(pf)$ configurations, in concert with the Chung-Wildenthal interaction[22] for the sd shell and the Millener-Kurath (MK) interaction[23] for all other two-body matrix elements. The resulting wave functions have been used previously in analyses of three-nucleon transfer on ^{15}N by Martz,[24] the β decay of ^{18}N to ^{18}O by Olness *et al.*,[25] and inelastic pion scattering on ^{18}O by Chakravarti *et al.*[6] We refer to other calculations for the negative-parity states of ^{18}O, as appropriate, in the following sections.

A. Excitation energies and wave functions

The predicted excitation energies, normalized to the 4.46-MeV 1^- level, a percentage decomposition of the wave functions into components of the form $p^{-1}(sd)^3$ [from which the percentage of $(sd)(pf)$ follows], where the $(sd)^3$ configurations have $T=\frac{1}{2}$ or $\frac{3}{2}$, and the dominant components in a weak-coupling decomposition of the wave functions are given in Table V. Configurations with $T=\frac{3}{2}$ for the sd shell play an important role in the wave functions of all states. The near degeneracy in energy of the $(sd)^3$ configurations with $T=\frac{1}{2}$ and $\frac{3}{2}$ may be understood in terms of the Bansal-French-Zamick model,[26] in which the particle-hole interaction is written in the greatly simplified form $V_{\mathrm{ph}}=\mathcal{A}+\mathcal{B}\mathbf{t}_p\cdot\mathbf{t}_h$. Then V_{ph} contributes $1.5\mathcal{B}$ to the energy difference between the aforementioned configurations, which, for a typical value of $\mathcal{B}=5$ MeV,[2] compensates for the energy difference be-

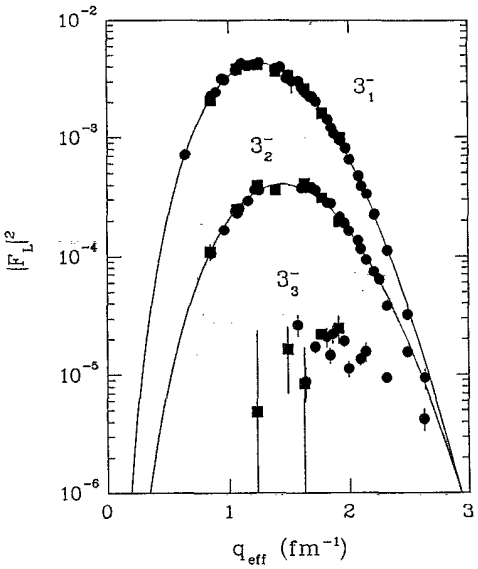

FIG. 4. Extracted Coulomb form factors for 3^- states in ^{18}O at excitation energies of 5.10 MeV (3_1^-), 6.40 MeV (3_2^-), and 8.29 MeV (3_3^-). See the caption to Fig. 3 for a description of the data points.

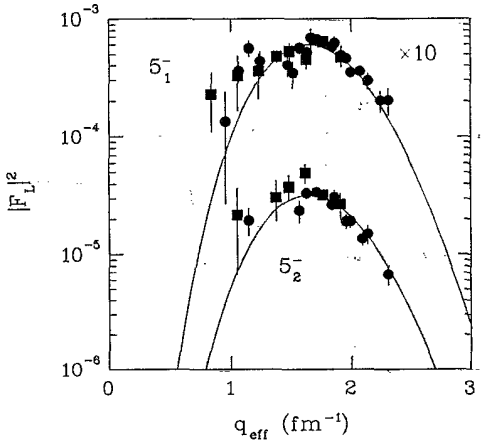

FIG. 5. Extracted Coulomb form factors for 5^- states in ^{18}O at excitation energies of 7.86 MeV (5_1^-) and 8.13 MeV (5_2^-). See the caption to Fig. 3 for a description of the data points.

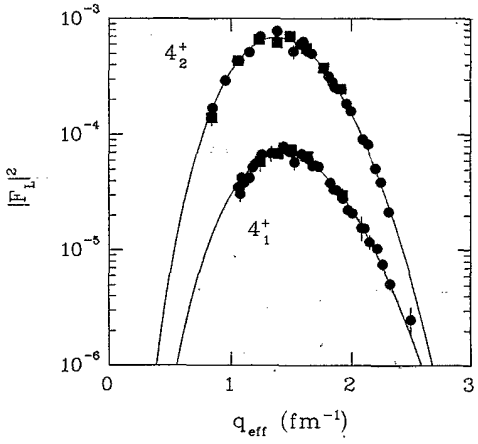

FIG. 6. Extracted Coulomb form factors for 4^+ states in ^{18}O at excitation energies of 3.56 MeV (4_1^+) and 7.12 MeV (4_2^+). See the caption to Fig. 3 for a description of the data points.

TABLE IV. Reduced transition probabilities [$B(CJ)\uparrow$ in units of $e^2\,\mathrm{fm}^{2J}$] for normal-parity levels in ^{18}O.

J_n^π	E_x (MeV)	This work[a]	Prior work[b]	Theory[c]
2_1^+	1.98	40.8(20)	44.8(13)[d]	47.6
2_2^+	3.92	21.1(11)	22.2(10)	15.4
2_3^+	5.26	28.5(17)	28.3(15)	27.6
3_1^-	5.10	1301(39)	1120(105)[e]	1256
3_2^-	6.40	40(9)		255
3_3^-	8.29	≤ 19		9
4_1^+	3.56	968(104)	904(90)	2.9×10^3
4_2^+	7.12	$1.29(10)\times10^4$	$1.31(6)\times10^4$	6.9×10^3
5_1^-	7.86	$3.54(64)\times10^4$		
5_2^-	8.13	$1.88(35)\times10^4$		

[a] The quoted uncertainties take into account the model dependency of our parametrization and the fact that there are no data points for $q_{\mathrm{eff}} < 0.65\ \mathrm{fm}^{-1}$.
[b] The experimental values are from Ref. 3 unless indicated otherwise.
[c] The theoretical $B(C2)\uparrow$, $B(C3)\uparrow$, and $B(C4)\uparrow$ values are from Ref. 19, this work, and Ref. 4, respectively.

tween the lowest $T=\frac{3}{2}$ and $\frac{1}{2}$ $(sd)^3$ configurations (7.54 MeV in ^{19}F). Alternatively, ^{15}N with $[4^33]$ spatial symmetry can be coupled to $(sd)^3$ with either [3] or [21] symmetry to form states with the highest symmetry $[4^42]$, the latter coupling necessarily involving $(sd)^3$ configurations with both $T=\frac{3}{2}$ and $\frac{1}{2}$.

It can be noted from Table V that the lowest 1^-, 3^-, and 7^- eigenstates contain large components with a $p_{1/2}$ hole coupled to members of the ^{19}F ground-state band, which have large overlaps with ^{16}O+t cluster configurations, and that such strength is shared by the two 5^- levels $(p_{1/2}^{-1}\times\frac{9}{2}^+;\frac{1}{2}$ and $p_{1/2}^{-1}\times\frac{9}{2}^+;\frac{3}{2}$

TABLE V. Negative-parity wave functions for ^{18}O.

J_n^π	E_x (expt) (MeV)	E_x (theor) (MeV)	$p^{-1}(sd)^3_{T=1/2}$ (%)	$p^{-1}(sd)^3_{T=3/2}$ (%)	Wave function[a]
1_1^-	4.46	4.46[b]	91.8	6.3	$0.869(\frac{1}{2}\times\frac{1}{2})+0.265(\frac{3}{2}\times\frac{1}{2})-0.224(\frac{3}{2}\times\frac{5}{2})$
1_2^-	6.20	6.83	43.3	38.8	$-0.541(\frac{1}{2}\times\frac{3}{2})-0.473(\frac{1}{2}\times\frac{1}{2}^*)$
1_3^-	7.62	7.63	49.8	45.6	$-0.580(\frac{1}{2}\times\frac{3}{2})+0.524(\frac{1}{2}\times\frac{1}{2}^*)+0.230(\frac{3}{2}\times\frac{5}{2}^*)$
1_4^-	8.04	8.21	43.1	48.6	$-0.289(\frac{1}{2}\times\frac{1}{2})+0.372(\frac{1}{2}\times\frac{1}{2}_2)+0.573(\frac{1}{2}\times\frac{3}{2}^*)$ $-0.220(\frac{1}{2}\times\frac{1}{2}^*)-0.202(\frac{3}{2}\times\frac{5}{2}^*)$
3_1^-	5.10	4.67	78.7	17.8	$0.815(\frac{1}{2}\times\frac{5}{2})+0.312(\frac{1}{2}\times\frac{5}{2}^*)$
3_2^-	6.40	6.17	32.5	66.8	$-0.405(\frac{1}{2}\times\frac{5}{2})+0.751(\frac{1}{2}\times\frac{5}{2}^*)$
3_3^-	8.29	7.52	22.9	60.7	$-0.664(\frac{1}{2}\times\frac{5}{2}_2^*)$
5_1^-	7.86	7.20	61.2	36.3	$-0.716(\frac{1}{2}\times\frac{9}{2})-0.510(\frac{1}{2}\times\frac{9}{2}^*)$
5_2^-	8.13	7.73	46.4	51.4	$0.567(\frac{1}{2}\times\frac{9}{2})-0.641(\frac{1}{2}\times\frac{9}{2}^*)$
7_1^-	11.13	10.06	97.8	2.2	$0.970(\frac{1}{2}\times\frac{13}{2})$

[a] Notation: $p^{-1}(J_h)\times(sd)^3(J_p)_n$, where $n=1$ if J_p is not subscripted and an asterisk indicates that $T_p=\frac{3}{2}$. Only large components are listed. The 29 lowest weak-coupling states were obtained by diagonalizing the shell-model Hamiltonian with the cross-shell matrix elements set to zero and, for some states listed, substantial strength resides in higher states. The percentage of $(sd)(pf)$ strength may be deduced from columns 4 and 5.
[b] Normalized.

configurations are strongly mixed). These states are all strongly populated in the ^{15}N(^{6}Li,^{3}He)^{18}O reaction,[24] the two 5^- states with comparable cross sections, consistent with the calculated 3p-1h structure. In the simplest version of the SU_3 model, the $J=1,3,5,7$ states above are the natural-parity members of a $(\lambda\mu)=(61)$ band with $K=1$ and $S=0$, the energies of which go as $A+B[1+\beta(-)^J]J(J+1)$.[27]

The predicted spectrum has the correct number of negative-parity states (of both even and odd J) below about 8.5 MeV after normalization of the energy of the lowest state, which is underbound by about 1 MeV. While the MK interaction gives a reasonable overall account of non-normal-parity states in nuclei around ^{16}O, it fails to reproduce in detail certain critical p-h matrix elements. An example is afforded by the observation of Barker[28] that the incorrect ordering given by the MK interaction for the $p^{-1}_{1/2}d_{5/2}$ states in ^{16}N leads to related problems in describing simple $p^{-1}_{1/2}d^2_{5/2}$ states in ^{17}N and $p^{-1}_{1/2}d^3_{5/2}$ states in ^{18}N. The isospin average of the $p^{-1}_{1/2}d_{5/2}$ 2^- and 3^- p-h matrix elements may be deduced from the energies of $p^{-1}_{1/2}d^2_{5/2}(5;0)$ $\frac{11}{2}^-$ and $\frac{9}{2}^-$ states in ^{17}O or from $p^{-2}_{1/2}d^2_{5/2}(5;0)$ 6^+ and 5^+ states in ^{16}O, with concordant results.[29] The p-h matrix elements from this fit are compared with the MK matrix elements in Table VI. With the exception of the $3^-;1$ matrix element, the fitted matrix elements are more attractive than the MK matrix elements and increase $\mathcal{B}$ (the difference between spin-averaged $T=1$ and 0 p-h matrix elements) from 3.1 to 5.0 MeV. The fitted matrix elements, although not appropriate for use in full configuration-mixed shell-model calculations, are very useful for estimating the excitation energies of states for which the weak-coupling approximation is valid (often high-spin states). Such estimates are made for several $[p^{-1}_{1/2}d^3_{5/2}(J_dT_d)]JT$ weak-coupling states in Table VII, where the calculated energy $E_{\rm th}$ is given in terms of diagonal p-h matrix elements, mass excesses, and a Coulomb correction by

$$E_{\rm th}=E_{\rm ME}+\Delta E_C+\sum_{J_{\rm ph}T_{\rm ph}} a(J_{\rm ph}T_{\rm ph})E(J_{\rm ph}T_{\rm ph})\,, \qquad (12)$$

where $E_{\rm ME}={\rm ME}(A=15)+{\rm ME}(A=19)-{\rm ME}(^{16}{\rm O})-{\rm ME}(^{18}{\rm O})$. The energies calculated for the $2^-;2$ and $7^-;1$ configurations are close to the experimental values and a similar calculation for the lowest 0^- level gives 6.74 MeV, to be compared with the experimental energy of 6.88 MeV. Since the weak-coupling assumptions are rather good for these states and the 7^- state is linked in a band structure with 1^-, 3^-, and 5^- states, we conclude that the lowest negative-parity states in ^{18}O are mainly of 3p-1h character. The energies of the other $T=1$ configurations in Table VII are lowered considerably by using the fitted rather than the MK matrix elements.

TABLE VI. Comparison of fitted $p^{-1}_{1/2}d_{5/2}$ matrix elements (in MeV) with values given by the MK interaction. See Eq. (12) and the accompanying text for an explanation of the symbols.

	$E(20)$	$E(21)$	$E(30)$	$E(31)$
Fitted	−0.86	1.65	−4.78	1.95
MK	0.69	2.33	−2.12	2.02

To make a rough estimate of the energies at which the lowest $3\hbar\omega$ states may be expected, we note that 1^- states at 9.58 MeV in ^{16}O and 5.79 MeV in ^{20}Ne can be interpreted as bandheads for α-cluster states. These states, which in the shell model are linear combinations of $p^{-m}(sd)^3(pf)$ and $p^{-(m+1)}(sd)^5$ configurations transforming as $(9m)$, lie 3.5 and 5.8 MeV above the corresponding 0^+ α-cluster states $[p^{-m}\times^{20}{\rm Ne(g.s.)}]$. A linear interpolation puts the corresponding bandhead in ^{18}O at 8.3 MeV (or 6.4 MeV in ^{18}F, where candidate states with large α widths exist[30]). Alternatively, putting the 1^- states in ^{16}O and ^{18}O at the same energy above the respective α thresholds gives 8.6 MeV in ^{18}O. A broad 1^- state observed[31] at 9.0 MeV in β-delayed α emission from ^{18}N is a candidate, with a width comparable to that of the 9.58-MeV state in ^{16}O. A review of calculations that include α-cluster states as the basis is given by Furutani *et al.*[30] Relatively pure $p^{-(m+1)}(sd)^5$ states with the maximum spatial symmetry and $(8,m+2)$ SU_3 symmetry should also exist for $A\geq 17$ (e.g., for $m=0$, the $K^\pi=2^-$ band in ^{20}Ne). Ellis and Engeland[32] predict 5p-3h states around 10 MeV in ^{18}O in a weak-coupling model that, like our shell-model calculation, underbinds the 3p-1h states by ~1 MeV, making ~9 MeV a plausible energy for the first 5p-3h states.

TABLE VII. Energies of $[p^{-1}_{1/2}d^3_{5/2}(J_dT_d)]JT$ configurations in ^{18}O in terms of the $p^{-1}_{1/2}d_{5/2}$ particle-hole matrix elements. See Eq. (12) and the accompanying text for an explanation of the symbols. All energies are in MeV, $E_{\rm WC}=E_{\rm ME}+\Delta E_C$, where $\Delta E_C=\langle n^\pi_{\rm ph}\rangle c$ and we take $c=-0.47$ MeV. Here $\langle n^\pi_{\rm ph}\rangle$ is the average number of proton particle-hole pairs (Ref. 26).

J^π	T	$J_d;T_d$	$a(20)$	$a(21)$	$a(30)$	$a(31)$	$E_{\rm WC}$	$E_{\rm th}$	$E_{\rm expt}$
2^-	2	$\frac{5}{2};\frac{3}{2}$		$\frac{11}{6}$		$\frac{7}{6}$	$11.68+\frac{3}{4}c$	16.64	16.40[a]
7^-	1	$\frac{13}{2};\frac{1}{2}$		$\frac{1}{6}$	$\frac{1}{2}$	$\frac{7}{3}$	$8.78+c$	10.75	11.13[b]
5^-	1	$\frac{9}{2};\frac{3}{2}$	$\frac{1}{3}$	$\frac{1}{6}$	$\frac{5}{3}$	$\frac{5}{6}$	$14.07+\frac{1}{4}c$	7.60	
3^-	1	$\frac{5}{2};\frac{3}{2}$	$\frac{5}{9}$	$\frac{5}{18}$	$\frac{13}{9}$	$\frac{13}{18}$	$11.70+\frac{1}{4}c$	6.06	
2^-	1	$\frac{3}{2};\frac{3}{2}$	$\frac{2}{3}$	$\frac{1}{3}$	$\frac{4}{3}$	$\frac{2}{3}$	$11.81+\frac{1}{4}c$	6.59	

[a] Reference 15.
[b] Reference 24.

TABLE VIII. One-body density-matrix elements in SU_3 coupling for an $(sd)^2$ ground state and $1\hbar\omega$ negative-parity states in ^{18}O. The $p\rightarrow sd$ Z coefficients listed are OBDME reduced in spin but not isospin. Z amplitudes for $sd\rightarrow pf$ excitations are small; however, $Z_1^{(10)}(sd\rightarrow pf)$ amplitudes are required to calculate $B(C1)$ values: $Z_1^{(10)}(sd\rightarrow pf)=-Z_0^{(10)}(sd\rightarrow pf)=\sqrt{(2/5)}Z_0^{(10)}(p\rightarrow sd)$. The proton or neutron amplitudes are given by $Z_{p/n}=\sqrt{(1/2)}(Z_0\pm Z_1)$.

J_n^π	ΔT	$Z_{\Delta T}^{(10)}(\Delta S=0)$	$Z_{\Delta T}^{(21)}(\Delta S=0)$	$Z_{\Delta T}^{(10)}(\Delta S=1)$	$Z_{\Delta T}^{(21)}(\Delta S=1)$
1_1^-	0	−0.049 28	0.339 89	0.044 76	0.225 34
	1	0.052 26	0.312 25	0.067 63	0.239 10
1_2^-	0	0.160 10	0.445 37	0.094 93	0.151 79
	1	−0.135 35	0.018 73	−0.009 82	−0.110 09
1_3^-	0	0.002 99	−0.454 11	−0.025 72	−0.309 14
	1	−0.039 81	0.168 44	0.069 73	0.002 45
1_4^-	0	−0.120 20	0.125 75	−0.038 17	−0.059 75
	1	−0.034 79	−0.114 44	−0.041 53	−0.245 09
3_1^-	0		−0.612 60		−0.278 95
	1		−0.203 09		−0.176 90
3_2^-	0		−0.416 82		−0.160 99
	1		0.236 29		0.235 44
3_3^-	0		0.023 81		0.072 43
	1		0.080 68		0.062 33

B. Shell-model form factors

The shell-model form factors for harmonic-oscillator single-particle wave functions are given by the right-hand sides of Eqs. (6) and (7) with the single-nucleon form factor and the center-of-mass correction omitted. In our model with an $(sd)^2$ ground state and $1\hbar\omega$ excited states, for which the one-body density-matrix elements (OBDME) are listed in Table VIII, the form factors for $C1$ and $C3$ transitions depend essentially on the OBDME with $(\lambda\mu)=(21)$ and $\Delta S=0$; the $(\lambda\mu)=(10)$ amplitudes are constrained to be small since the $B(E1)$ values are small (Table III) and the small $sd\rightarrow pf$ amplitudes contribute to $C1$ or $C3$ transitions only if an effective charge for neutrons is introduced. Then the $C1$ and $C3$ form factors both have the form $y^{3/2}e^{-y}$. However, the PG coefficients listed in Table I and the discussion in Sec. IV indicate the need for contributions other than $p\rightarrow sd$ excitations. As an example, we consider admixtures of $p\rightarrow sdg$ excitations, which introduce OBDME with $(\lambda\mu)=(30)$ and (41), and we can write

$$F_{C1}=\frac{1}{Z}\left[\frac{2}{5}\right]^{1/2}y^{1/2}e^{-y}\left[Z^{(21)}y-\sqrt{20}Z^{(10)}\left[1-\frac{y}{2}\right]-\sqrt{12}Z^{(30)}\left[y-\frac{y^2}{3}\right]\right], \tag{13}$$

$$F_{C3}=\frac{1}{Z}\left[\frac{8}{5}\right]^{1/2}y^{3/2}e^{-y}\left[Z^{(21)}-\sqrt{2}Z^{(30)}\left[1-\frac{y}{3}\right]\right], \tag{14}$$

$$F_{C5}=\frac{1}{Z}\left[\frac{32}{189}\right]^{1/2}y^{5/2}e^{-y}[Z^{(41)}], \tag{15}$$

where $Z^{(\lambda\mu)}=e_0Z_0^{(\lambda\mu)}+e_1Z_1^{(\lambda\mu)}$, $e_0=1+\delta e_p+\delta e_n$, and $e_1=1+\delta e_p-\delta e_n$. Here $Z^{(41)}$ terms, which enter with coefficients $\sqrt{2/21}$ and $\sqrt{4/27}$ for $C1$ and $C3$, respectively, have been dropped.

To reproduce the peak form factors of 6×10^{-5} and 3.2×10^{-5} for the two 5^- states in Fig. 5 requires $Z^{(41)}=0.213$ and 0.156, respectively ($q=1.65$ fm^{-1}, $b=1.879$ fm), i.e., a total of 7% of the total isoscalar $p\rightarrow sdg$ strength.

For many strong $C3$ excitations in nuclei around ^{16}O, effective charges $e_0=1.63$ and $e_1=0.7$, when used with $0\hbar\omega$ wave functions for ground states and $1\hbar\omega$ wave functions for excited states, reproduce very well the magnitude of form factors [and hence $B(C3)$ values]. In particular, this is true for the oxygen isotopes.[2,6] Much of the enhancement represented by the effective charges can be attributed to random-phase-approximation (RPA) correlations (2p-2h $\cdots$) within the $p(sd)$ space,[33] well illustrated in the extension of the schematic model from Tamm-Dancoff approximation (TDA) to RPA.[34] At this level the shape of the form factor remains unchanged; however, an expansion of the model space[35] to include $3\hbar\omega$ single-particle excitations further strengthens the low-lying octupole excitation and brings in terms such as the $Z^{(30)}(1-\frac{1}{3}y)$ term in Eq. (14), which give rise to the negative A_1 coefficient in Table I and cause the form factor to fall off faster at high q (see Fig. 4 and Ref. 36).

When the shell-model $Z^{(21)}$ amplitudes for the 3_1^- level are used with $e_0=1.63$ and $e_1=0.7$, we find a peak longi-

tudinal form factor of 4.6×10^{-3}, a value that is increased slightly when the $sd\rightarrow pf$ amplitudes are included with the same effective charges. The transverse form factor peaks at 2.5×10^{-5} (convection current from the continuity equation and magnetization current quenched by a factor of 0.7), which is consistent with the experimental observation that the transverse form factor must be small. Figure 7 compares the longitudinal and transverse shell-model form factors for the 3_1^- level with the measured values. The shell-model form factor for the 3_2^- level peaks at 9×10^{-4}, which is a factor of two larger than the experimental form factor shown in Fig. 4; however, the amplitudes involving higher orbits, which are necessary to account for the shape of the form factor (the fitted A_0 and A_1 coefficients in Table I are of the same sign), probably interfere destructively with the $p\rightarrow sd$ amplitude in the A_0 coefficient. The 3_3^- form factor is predicted to peak at 3×10^{-5}, which is consistent with the data.

The $C1$ form factor predicted for the lowest 1^- state (shown in Fig. 8) does not resemble the measured form factor. It necessarily has the shape of a $C3$ form factor and the peak magnitude of 3.8×10^{-4} is much less than 1.7×10^{-3} for the measured form factor; however, as was pointed out by Millener *et al.*[36] and can be seen from Eq. (12), the $p\rightarrow sdg$ (30) amplitudes are particularly effective for $C1$ transitions. Very good agreement with the A_1 and A_2 coefficients in Table I is obtained by choosing $Z^{(30)}=-0.388$ together with $Z^{(21)}=0.652$ from our shell-model calculation. The effect of such an admixture on the transition densities is to move the node outward, as can be seen by comparing the experimentally derived transition density for the 1_1^- level in Fig. 2(a) with that for the 1_4^- level in Fig. 2(b) (transition densities for the 1^- levels are discussed at some length in Refs. 6 and 36). The predicted transverse form factor (also shown in Fig. 8), with no quenching of the magnetization current, peaks at $q=1.42$ fm^{-1} with a magnitude of 7.2×10^{-5}. With a quenching factor of 0.7, the peak magnitude drops to 4.8×10^{-5}, which is still larger than the measured form factor in Fig. 3(b). The convection and magnetization current contributions interfere constructively. Adding the $p\rightarrow sdg$ $Z^{(30)}$ amplitude reduces the convection current and the peak transverse form factor drops to 3.6×10^{-5}.

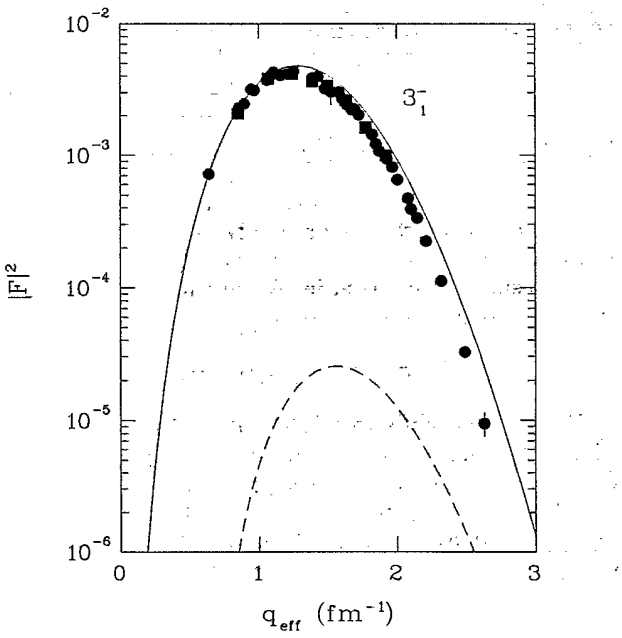

FIG. 7. Shell-model Coulomb (solid line) and transverse electric (dashed line) form factors for the 3_1^- state in ^{18}O at 5.10 MeV. See the caption to Fig. 3 for a description of the data points.

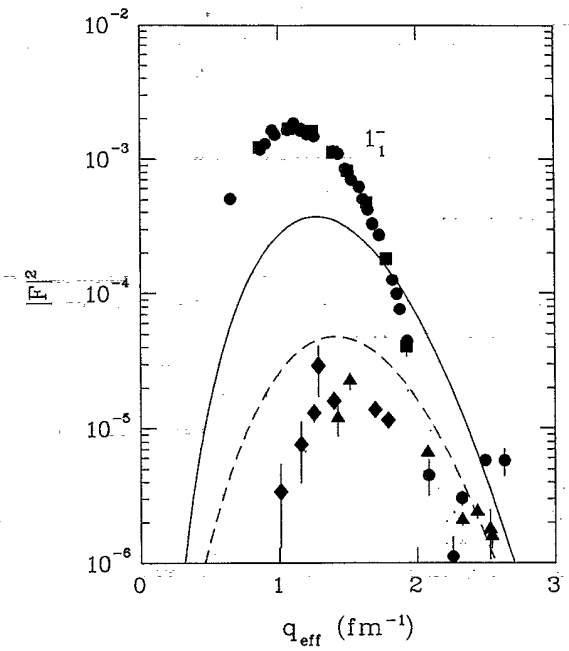

FIG. 8. Shell-model Coulomb (solid line) and transverse electric (dashed line) form factors for the 1_1^- state in ^{18}O at 4.46 MeV. See the caption to Fig. 3 for a description of the data points.

The 6.20-MeV 1^- level has an unusual longitudinal form factor and it would be interesting to have experimental measurements at lower q. The predicted $C1$ form factor again has the $C3$ shape with a maximum value of about 1.7×10^{-4}. The predicted transverse form factor is negligibly small because the magnetization current contribution, which is itself weak, interferes destructively with the convection-current contribution. This prediction at least is consistent with the data but it is clear that the contributions from higher orbits play an important role. The $B(E1)$ values for the 1_3^- and 1_4^- model states are much larger than the experimental values for the 7.62- and 8.04-MeV states. For the 1_4^- model state, the $Z^{(21)}$ proton amplitude is extremely small and its longitudinal form factor exhibits the "giant-dipole" shape with a maximum of 3.4×10^{-4} at $q\sim0.6$ fm^{-1}. As we discuss below, the 1_3^- model state might better be identified with the 8.04-MeV level. Indeed, the model state has quite a strong isoscalar (21) amplitude $Z_0^{(21)}=-0.454$, which is comparable to those of the first two 1^- model states;

however, the $C1$ form factor reaches only 5.7×10^{-5}, and, even without the canceling isovector amplitude (neutron excitation dominates), the isoscalar amplitude gives a peak longitudinal form factor of only 1.8×10^{-4}. Thus, although the measured form factor for the 8.04-MeV level has precisely the shape expected for a $p\rightarrow sd$ (21) transition, its magnitude is much greater than anything except a strong proton transition can produce. Since the proton strength resides in the first two 1^- model states, it appears that contributions from higher orbits are again required, there being no reason that they cannot produce a form factor with the observed shape. The predicted transverse form factors have maxima of 2.7×10^{-5}, at $q=1.0$ fm^{-1} for the 1_3^- model state (comparable and constructive convection and magnetization currents) and at $q=1.6$ fm^{-1} for the 1_4^- state (all magnetization).

The shell-model calculations predict that Z_p (the proton OBDME) for the $p\rightarrow sd$ transition corresponding to the SU_3 (21) amplitude is very small for the 1_4^- model state at 8.21 MeV but is of modest size for the 1_3^- model state at 7.63 MeV (see Table VIII). The situation is reversed for the corresponding isovector $\Delta S=1$ amplitudes; hence, the observation that the observed 1_3^- state at 7.62 MeV has a small longitudinal form factor and a significant transverse form factor may be understood if we identify this state with the predicted state at 8.21 MeV. There is independent evidence from the ^{19}F$(d,^3$He$)^{18}$O reaction[37] that the 1_4^- model state, with a modest amplitude for $p_{1/2}$ pick up (see Table V), should be identified with the 7.62-MeV level, which is a member of an unresolved pair (including as well the 7.77-MeV 2^- level) seen at 7.67 MeV. The strength C^2S (mostly $p_{1/2}$) for our 1_4^- and 2_3^- model states relative to the sum of strengths for the peaks at 4.46 MeV (1_1^-) and 6.27 MeV (1_2^- and 2_2^-) is in good agreement with that observed; however, the model predicts that most of the $p_{1/2}$ pickup strength is to the 1_1^- state, while the observed strength is split between the first and second 1^- states in the ratio 2:1. The (π,π') data[6] and the $M1$ decays[38] of the analog 1^- states in ^{18}F to the 1.08-MeV 0^- state similarly indicate a need to mix the 1_1^- and 1_2^- model states.[39]

VI. SUMMARY

In this work we have presented the results of high-resolution form-factor measurements for four 1^- states, three 3^- states, and two 5^- states in ^{18}O. These are all of the known states in ^{18}O below 9 MeV with normal-negative parity. A Rosenbluth separation of the longitudinal and transverse components was achieved by fitting the data with polynomial-times-Gaussian parameterizations motivated by harmonic-oscillator wave functions; the oscillator parameter was determined to be 1.879 ± 0.023 fm by fitting form-factor measurements for the nine negative-parity states and for four 2^+ states and two 4^+ states simultaneously. Except for the lowest three 1^- states, the form factors were found to be completely longitudinal, within experimental uncertainties. The variation of the Coulomb form factors with momentum transfer indicates the significance of $3\hbar\omega$ admixtures in the wave functions of the first two 1^- states, the second 3^- state, and the first two 5^- states. As such, the data critically test shell-model descriptions of the negative-parity states in ^{18}O.

The effects of meson-exchange currents are expected to be small over the momentum-transfer range (0.5–2.5 fm^{-1}) of our measurements. The most important contributions to the nuclear matrix elements are from the long-range exchange of pions. In the work of Dubach, Koch, and Donnelly,[40] the charge density remains unchanged and only the isovector part of the transverse form factor is modified; thus, our conclusions involving the $C1$, $C3$, and $C5$ form factors are not expected to alter by considerations of exchange currents. The effects of meson-exchange currents on the small $E1$ form factors will probably be more significant; however, the effects are still expected to be small in the momentum-transfer range considered here.

The effect of $3\hbar\omega$ admixtures of 1p-1h nature, such as the $p\rightarrow sdg$ excitations emphasized in Sec. V A, can probably be treated perturbatively.[41–43] In fact, Erikson[43] has made estimates for ^{16}O and finds admixtures of the order of 9% for the 6.13-MeV 3_1^- level and somewhat less for the 7.12-MeV 1_1^- level. It is clear from the discussion in Sec. V that it is important to refine the cross-shell interaction to obtain a better description of configuration mixing involving the dominant 3p-1h components of the low-lying negative-parity levels. It is also of interest to investigate the effects of including the $p^{-3}(sd)^5$ and $p^{-2}(sd)^3(pf)$ configurations discussed at the end of Sec. V A, perhaps by using a weak-coupling basis. These configurations can be excited via the 4p-2h components in the ground state and related to the corresponding transition strengths in ^{20}Ne, where the (e,e') data[44] can be adequately described by $1\hbar\omega$ calculations analogous to those described here for ^{18}O.[45] Their effect is unlikely to be as important as that of the 4p-2h configurations for the positive-parity states since the dominant $(sd)^2\rightarrow p^{-1}(sd)^3$ transitions involve protons and are not weak [cf. $(sd)^2\rightarrow(sd)^2$]. Also, the $3\hbar\omega$ states lie above the $1\hbar\omega$ states of interest, in contrast to be interleaving of the $0\hbar\omega$ and $2\hbar\omega$ configurations.

ACKNOWLEDGMENTS

The authors thank the technical staff at the MIT-Bates Linear Accelerator Center for their support during the experiment. This work was supported in part by the National Science Foundation under Grant No. PHY-8902479 and by the U.S. Department of Energy under Contracts No. DE-AC02-76ER03069 and DE-AC02-76CH00016 and Grant No. DE-FG05-86ER40285.

[a]Present address: IBM Corporation, General Technology Division, Hopewell Junction, NY 12533.

[b]Present address: Department of Physics, College of William & Mary, Williamsburg, VA 23185.

[c]Present address: Department of Physics, University of New Hampshire, Durham, NH 03824.

[d]Present address: Department of Physics, University of Washington, Seattle, WA 98195.

[e]Present address: Los Alamos National Laboratory, Los Alamos, NM 87545.
[f]Present address: Department of Physics and Astronomy, University of Maryland, College Park, MD 20742.
[g]Present address: Department of Physics, University of Kentucky, Lexington, KY 40506.
[h]Present address: Department of Physics, University of Virginia, Charlottesville, VA 22901.
[i]Present address: Tektronics Inc., Beaverton, OR 97077.
[j]Present address: Department of Physics, Luther College, Decorah, IA 52101.
[k]Retired.

[1]T. N. Buti, J. Kelly, W. Bertozzi, J. M. Finn, F. W. Hersman, C. Hyde-Wright, M. V. Hynes, M. A. Kovash, S. Kowalski, R. W. Lourie, B. Murdock, B. E. Norum, B. Pugh, C. P. Sargent, W. Turchinetz, and B. L. Berman, Phys. Rev. C **33**, 755 (1986).

[2]D. M. Manley, B. L. Berman, W. Bertozzi, T. N. Buti, J. M. Finn, F. W. Hersman, C. E. Hyde-Wright, M. V. Hynes, J. J. Kelly, M. A. Kovash, S. Kowalski, R. W. Lourie, B. Murdock, B. E. Norum, B. Pugh, and C. P. Sargent, Phys. Rev. C **36**, 1700 (1987).

[3]B. E. Norum, M. V. Hynes, H. Miska, W. Bertozzi, J. Kelly, S. Kowalski, F. N. Rad, C. P. Sargent, T. Sasanuma, W. Turchinetz, and B. L. Berman, Phys. Rev. C **25**, 1778 (1982).

[4]D. M. Manley, D. J. Millener, B. L. Berman, W. Bertozzi, T. N. Buti, J. M. Finn, F. W. Hersman, C. E. Hyde-Wright, M. V. Hynes, J. J. Kelly, M. A. Kovash, S. Kowalski, R. W. Lourie, B. Murdock, B. E. Norum, B. Pugh, and C. P. Sargent, Phys. Rev. C **41**, 448 (1990).

[5]J. L. Groh, R. P. Singhal, H. S. Caplan, and B. S. Dolbilkin, Can. J. Phys. **49**, 2743 (1971).

[6]S. Chakravarti, D. Dehnhard, M. A. Franey, S. J. Seestrom-Morris, D. B. Holtkamp, C. L. Blilie, A. C. Hayes, C. L. Morris, and D. J. Millener, Phys. Rev. C **35**, 2197 (1987).

[7]W. Bertozzi, M. V. Hynes, C. P. Sargent, C. Creswell, P. C. Dunn, A. Hirsch, M. Leitch, B. Norum, F. N. Rad, and T. Sasanuma, Nucl. Instrum. Methods **141**, 457 (1977).

[8]W. Bertozzi, M. V. Hynes, C. P. Sargent, W. Turchinetz, and C. Williamson, Nucl. Instrum. Methods **162**, 211 (1979).

[9]T. DeForest, Jr. and J. D. Walecka, Adv. Phys. **15**, 1 (1966).

[10]G. R. Hammerstein, R. H. Howell, and F. Petrovich, Nucl. Phys. **A213**, 45 (1973).

[11]See AIP Document no. PAPS PRVCA-43-2147-22 for 22 pages containing a complete tabulation of the data described in this paper. Order by PAPS number and journal reference from American Institute of Physics Auxiliary Publication Service, 335 E. 45th St., New York, NY 10017. The price is $1.50 for each microfiche or $5.00 for photocopies of up to 30 pages and $0.15 for each page of 30 pages. Airmail additional. Make checks payable to American Institute of Physics.

[12]See, for example, R. S. Willey, Nucl. Phys. **40**, 529 (1963).

[13]B. A. Brown, W. Chung, and B. H. Wildenthal, Phys. Rev. C **22**, 774 (1980).

[14]H. Miska, B. Norum, M. V. Hynes, W. Bertozzi, S. Kowalski, F. N. Rad, C. P. Sargent, T. Sasanuma, and B. L. Berman, Phys. Lett. **83B**, 165 (1979).

[15]F. Ajzenberg-Selove, Nucl. Phys. **A475**, 1 (1987).

[16]F. D. Lee, R. W. Krone, and F. W. Prosser, Jr., Nucl. Phys. **A96**, 209 (1967).

[17]M. Hass, Z. Shkedi, D. F. H. Start, Y. Wolfson, and Y. S. Horowitz, Nucl. Phys. **A220**, 217 (1974).

[18]M. Gai, R. Keddy, D. A. Bromley, J. W. Olness, and E. K. Warburton, Phys. Rev. C **36**, 1256 (1987); see also R. K. Bhowmik, W. D. M. Rae, and B. R. Fulton, Phys. Lett. **136B**, 149 (1984).

[19]A. C. Hayes, P. J. Ellis, and D. J. Millener (unpublished).

[20]G. C. Ball, T. K. Alexander, W. G. Davies, J. S. Forster, and I. V. Mitchell, Nucl. Phys. **A377**, 268 (1982); see also S. Raman, C. H. Malarkey, W. T. Milner, C. W. Nestor, Jr., and P. H. Stelson, At. Data Nucl. Data Tables **36**, 1 (1987).

[21]R. D. Lawson, F. J. D. Serduke, and H. T. Fortune, Phys. Rev. C **14**, 1245 (1976).

[22]W. Chung, Ph.D. dissertation, Michigan State University, 1976.

[23]D. J. Millener and D. Kurath, Nucl. Phys. **A255**, 315 (1975).

[24]L. M. Martz, Ph.D. dissertation, Yale University, 1978.

[25]J. W. Olness, E. K. Warburton, D. E. Alburger, C. J. Lister, and D. J. Millener, Nucl. Phys. **A373**, 13 (1982).

[26]R. Bansal and J. B. French, Phys. Lett. **11**, 145 (1964); L. Zamick, *ibid.* **19**, 580 (1965).

[27]M. Harvey, Adv. Nucl. Phys. **1**, 67 (1968).

[28]F. C. Barker, Aust. J. Phys. **37**, 17 (1984).

[29]D. J. Millener, Argonne National Laboratory Report No. ANL/PHY-89/1, 1989, p. 47.

[30]H. Furutani, H. Kanada, T. Kaneko, S. Nagata, H. Nishioka, S. Okabe, S. Saito, T. Sakuda, and M. Seya, Prog. Theor. Phys. Suppl. **68**, 193 (1980); see also P. Descouvemont and D. Baye, Phys. Rev. C **31**, 2274 (1985).

[31]Z. Zhao, M. Gai, B. J. Lund, S. L. Rugari, D. Mikolas, B. A. Brown, J. A. Nolan, Jr., and M. Samuel, Phys. Rev. C **39**, 1985 (1989).

[32]P. J. Ellis and T. Engeland, Nucl. Phys. **A144**, 161 (1970).

[33]V. Gillet and N. Vinh Mau, Nucl. Phys. **54**, 321 (1964); **57**, 698(E) (1964).

[34]G. E. Brown, *Unified Theory of Nuclear Models and Forces* (North-Holland, Amsterdam, 1967).

[35]M. W. Kirson, Phys. Lett. **108B**, 237 (1982).

[36]D. J. Millener, D. I. Sober, H. Crannell, J. T. O'Brien, L. W. Fagg, S. Kowalski, C. F. Williamson, and L. Lapikás, Phys. Rev. C **39**, 14 (1989).

[37]G. Th. Kaschl, G. J. Wagner, G. Mairle, U. Schmidt-Rohr, and P. Turek, Nucl. Phys. **A155**, 417 (1970).

[38]I. Berka, K. P. Jackson, C. Rolfs, A. M. Charlesworth, and R. E. Azuma, Nucl. Phys. **A288**, 317 (1977); J. C. Sens, S. M. Refaei, and A. Pape, Phys. Rev. C **18**, 2007 (1978).

[39]A. C. Hayes, D. A. Bromley, and D. J. Millener (unpublished).

[40]J. Dubach, J. H. Koch, and T. W. Donnelly, Nucl. Phys. **A271**, 279 (1976).

[41]A. Arima, P. Manakos, and D. Strottman, Phys. Lett. **60B**, 1 (1975).

[42]B. Castel, Y. Okuhara, and H. Sagawa, Phys. Rev. C **42**, 1203 (1990).

[43]T. Erikson, Nucl. Phys. **A211**, 105 (1973).

[44]R. P. Singhal, H. S. Caplan, J. R. Moreira, and T. E. Drake, Can. J. Phys. **51**, 2125 (1973).

[45]D. J. Millener (unpublished).